United States Department of Commerce
Technology Administration
National Institute of Standards and Technology

NIST Technical Note 1371

Effective Medium Theory for Ferrite-Loaded Materials

Richard G. Geyer
Joseph Mantese
James Baker-Jarvis

Effective Medium Theory for Ferrite-Loaded Materials

Richard G. Geyer
Joseph Mantese
James Baker-Jarvis

Electromagnetic Fields Division
Electronics and Electrical Engineering Laboratory
National Institute of Standards and Technology
325 Broadway
Boulder, Colorado 80303-3328

October 1994

U.S. DEPARTMENT OF COMMERCE, Ronald H. Brown, Secretary
TECHNOLOGY ADMINISTRATION, Mary L. Good, Under Secretary for Technology
NATIONAL INSTITUTE OF STANDARDS AND TECHNOLOGY, Arati Prabhakar, Director

National Institute of Standards and Technology Technical Note
Natl. Inst. Stand. Technol., Tech. Note 1371, 24 pages (October 1994)
CODEN:NTNOEF

U.S. GOVERNMENT PRINTING OFFICE
WASHINGTON: 1994

For sale by the Superintendent of Documents, U.S. Government Printing Office, Washington, DC 20402-9325

Contents

EFFECTIVE MEDIUM THEORY FOR FERRITE-LOADED MATERIALS

Richard G. Geyer[1], Joseph Mantese[2], and James Baker-Jarvis[1]

A ferrite-loaded composite medium is modeled by spherical inclusions spaced equally on a cubic lattice within a host matrix. Both the inclusions and host matrix may be magnetically permeable and possess dielectric and magnetic loss. The ferrite-loaded medium may be considered to consist of excited Hertzian electric and magnetic dipole sources. Effective medium rules of a modified Maxwell-Garnett form can be derived by analysis of plane-wave propagation through the composite. These rules do not yield symmetric characterization of two-phase media. They are compared with other effective medium theories (Lorentz-Lorenz, Maxwell-Garnett, and Bruggeman) and broadband coaxial transmission line data measured on ferrite-loaded titanates of known composition. The modified Maxwell-Garnett rules give both lower and upper bounds for the effective permittivities and permeabilities of the composite and yield accurate estimates of bulk electric and magnetic properties for low volumetric inclusion loading. The Bruggeman formalism yields the best predictive permittivity and permeability values when volumetric percentages of the inclusions and host matrix are approximately equal. Generally, maximal magnetic loss factors occur at a frequency where the static initial permeability decreases by a factor of one-half, and the relaxation frequency for ferrite composites increases with decreasing static initial permeability.

Key words: composites; effective medium; ferrites; microwave; mixing rules; permeability; permittivity

---

[1]Electromagnetic Fields Division

[2]General Motors Research Laboratories, 30500 Mound Road, Warren, MI 48090-9055

1 Introduction

Dielectric and magnetic composite materials have complex permittivity and permeability properties that are determined by their constituents. Frequently, spectral characteristics for the dielectric and magnetic properties that differ from those of individual constituent materials are needed. Hence it is necessary to produce a material whose electromagnetic properties follow some specified behavior. This may be accomplished by either loading a material or by making multiphase mixtures. The loading constituent may take the form of small spheres, ellipsoids, platelets, rods, or other shapes. The bulk properties of the composite will depend on the alignment of the loading particles and therefore may be dielectrically or magnetically anisotropic. The loading particles may also interact with each other. Thus, the size, shape, and alignment of the loading material particles enter into mathematical formalisms describing the electromagnetic behavior.

Effective medium theory has been studied for many years [1-6]. In this paper we evaluate the applicability of coupled electric- and magnetic-field integral equation solutions for the effective propagation constant and impedance of a two-phase mixture that is modelled by a uniform lattice of spheres embedded in a matrix [4]. In the formalism the spherical loading particles and matrix may have any dielectric or magnetic properties. The inclusions may be electrically and magnetically penetrable or nonpenetrable. For example, porosity in a polycrystalline ceramic or expanded polymer may be modeled by lossless inclusions whose relative permittivity is unity. Similarly, the microscopic structure of various metal glasses, colloidal solutions, and metallic films may be modeled by nonpenetrable metallic inclusions. Calculated dielectric and magnetic properties corresponding to certain assumed microstructures may be compared with those observed in laboratory measurements. In the limiting case where the sphere radius is much less than the wavelength in the matrix, the mathematical formalism simplifies markedly.

2 Theory

2.1 Modified Maxwell-Garnett Formulation

Consider the case (figure 1) in which the matrix material, characterized by ϵ^*_m, μ^*_m, is loaded by spherical particles of radius a that have complex permittivity and permeability ϵ^*_p, μ^*_p and that are equally spaced in a cubic lattice with distance d between particle centers. Now allow a plane wave of unit amplitude, polarized in the x- direction and propagating in the z- direction, to be incident upon the matrix loaded with

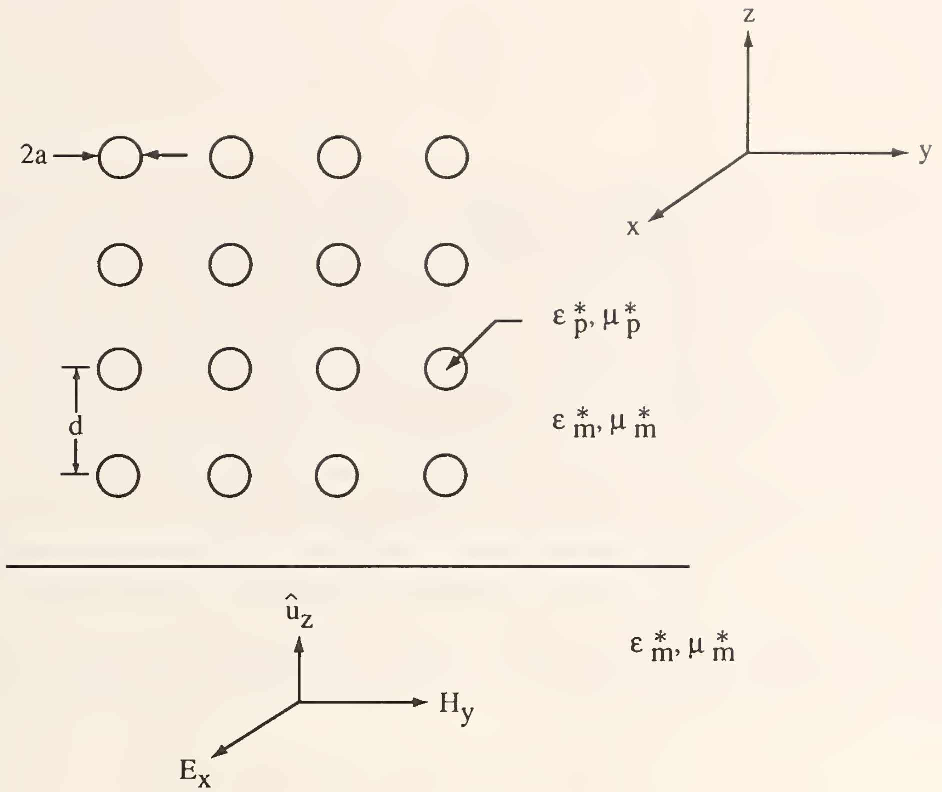

Figure 1. Uniform lattice of spheres in dielectric permeable matrix.

the spherical particles. Then, for $e^{j\omega t}$ time dependence,

$$E_x = e^{-\gamma_m z}, \tag{1}$$

and

$$H_y = -\frac{1}{j\omega\mu^*_m}\frac{\partial E_x}{\partial z} = \left(\frac{\epsilon^*_m}{\mu^*_m}\right)^{\frac{1}{2}} e^{-\gamma_m z}, \tag{2}$$

where $\gamma_m = jk_m = j\omega\sqrt{\mu^*_m\epsilon^*_m}$, $\mu^*_m = \mu_0\mu^*_{r,m} = \mu_0(\mu'_{r,m} - j\mu''_{r,m})$, $\epsilon^*_m = \epsilon_0\epsilon^*_{r,m}$ $= \epsilon_0(\epsilon'_{r,m} - j\epsilon''_{r,m})$, and $\mu^*_{r,m}$, $\epsilon^*_{r,m}$ denote the relative complex permeability and complex permittivity of the matrix. The permittivity and permeability of free space are $\epsilon_0 = 8.854 \times 10^{-12}$ F/m and $\mu_0 = 4\pi \times 10^{-7}$ H/m. At $z = 0$, the reflection coefficient Γ is given by

$$\Gamma = \frac{(\mu^*_{eff}/\epsilon^*_{eff})^{\frac{1}{2}} - (\mu^*_m/\epsilon^*_m)^{\frac{1}{2}}}{(\mu^*_{eff}/\epsilon^*_{eff})^{\frac{1}{2}} + (\mu^*_m/\epsilon^*_m)^{\frac{1}{2}}}, \tag{3}$$

where the reflected wave is assumed to be a plane wave and where fields propagate in the loaded material with a *bulk* or *effective* propagation factor $k_{eff} = \omega\sqrt{\epsilon^*_{eff}\mu^*_{eff}}$.

The field at a given particle inclusion location (u, v, w) is the sum of the incident field and a scattered field composed of all fields reradiated by the rest of the particles. We may assume that the total exciting field is a function of only the coordinate w, since all particles in the plane $z = w$ are affected in the same way; that is $E_x^t = E(w)$ and $H_y^t = H(w)$. At the center of a loading particle, all components of the scattered field may be considered negligible. If we further allow the particle radius to be sufficiently small, the field can be considered constant over its volume. Hence, the effect of a loading particle can be found from a consideration of the scattering due to a sphere in a medium characterized by (ϵ_m^*, μ_m^*) that is excited by $E(w)$ and $H(w)$.

In general, we may consider the ferrite-loaded medium to consist of excited electric and magnetic dipole sources [5], which may be described in terms of Hertz vectors, $\vec{\Pi}^e$ and $\vec{\Pi}^m$. In the matrix both Hertz vectors are multiples of $e^{-jk_m r}/r$, where r is the distance from the source point (u, v, w) to the field point (x, y, z). The fields in the matrix may be expressed as

$$\vec{E} = \nabla(\nabla \cdot \vec{\Pi}^e) + k_m^2 \vec{\Pi}^e - j\omega\mu_m^* \nabla \times \vec{\Pi}^m, \tag{4}$$

and

$$\vec{H} = \nabla(\nabla \cdot \vec{\Pi}^m) + k_m^2 \vec{\Pi}^m + j\omega\epsilon_m^* \nabla \times \vec{\Pi}^e. \tag{5}$$

The electric Hertz vector has only an x-component and the magnetic Hertz vector only a y-component, so that

$$E_x = [C(\frac{\partial^2}{\partial x^2} + k_m^2) + j\omega\mu_m^* D \frac{\partial}{\partial z}] \frac{e^{-jk_m r}}{r}, \tag{6}$$

and

$$H_y = [D(\frac{\partial^2}{\partial y^2} + k_m^2) + j\omega\epsilon_m^* C \frac{\partial}{\partial z}] \frac{e^{-jk_m r}}{r}, \tag{7}$$

where C and D are determined by continuity of tangential field components at the surface of a sphere in the matrix. Equations (4) and (5) must be written in spherical coordinates before application of continuity conditions. The contribution to the scattered electric field from $\vec{\Pi}^e$ may be written in spherical coordinates as

$$\begin{aligned} \nabla(\nabla \cdot \vec{\Pi}^e) + k_m^2 \vec{\Pi}^e &= \hat{u}_r[\sin\theta\cos\phi\left(\frac{\partial^2 U}{\partial r^2} + k_m^2 U\right) + \frac{\cos\theta\cos\phi}{r^2}\left(r\frac{\partial^2 U}{\partial r \partial\theta} - \frac{\partial U}{\partial\theta}\right) \\ &+ \frac{\sin\phi}{r^2\sin\theta}\left(\frac{\partial U}{\partial\phi} - r\frac{\partial^2 U}{\partial r\partial\phi}\right)] \end{aligned}$$

$$
\begin{aligned}
&+ \quad \frac{\hat{u}_\theta}{r^2}[r\cos\phi\left(\sin\theta\frac{\partial^2 U}{\partial r\partial\theta}) + \cos\theta\frac{\partial U}{\partial r}\right) \\
&+ \quad \cos\phi\left(\cos\theta\frac{\partial^2 U}{\partial\theta^2} - \sin\theta\frac{\partial U}{\partial\theta}\right) - \frac{\sin\phi}{\sin^2\theta}\left(\sin\theta\frac{\partial^2 U}{\partial\phi\partial\theta} - \cos\theta\frac{\partial U}{\partial\phi}\right) \\
&+ \quad k_m^2 r^2 U\cos\theta\cos\phi] + \frac{\hat{u}_\phi}{r^2}[r\left(\cos\phi\frac{\partial^2 U}{\partial r\partial\phi} - \sin\phi\frac{\partial U}{\partial r}\right) \\
&+ \quad \cot\theta\left(\cos\phi\frac{\partial^2 U}{\partial\theta\partial\phi} - \sin\phi\frac{\partial U}{\partial\theta}\right) - \csc^2\theta\left(\sin\phi\frac{\partial^2 U}{\partial\phi^2} + \cos\phi\frac{\partial U}{\partial\phi}\right) \\
&- \quad k_m^2 r^2 U\sin\phi], \qquad (8)
\end{aligned}
$$

where $\hat{u}_r, \hat{u}_\theta, \hat{u}_\phi$ are unit vectors in spherical coordinates, $\vec{\Pi}^e = \hat{u}_x U$, and U is a multiple of $e^{-jk_m r}/r$. The contribution to the electric field from $\vec{\Pi}^m$ is given by $-j\omega\mu_m^* \nabla \times \vec{\Pi}^m$, where

$$
\begin{aligned}
\nabla \times \vec{\Pi}^m &= \frac{\hat{u}_r}{r}\left[\frac{\partial V}{\partial\theta} - \cot\theta\sin\phi\frac{\partial V}{\partial\phi}\right] \\
&- \frac{\hat{u}_\theta}{r}\left[\sin\phi\frac{\partial V}{\partial\phi} + r\cos\phi\frac{\partial V}{\partial r}\right] \\
&+ \frac{\hat{u}_\phi}{r}\left[\sin\phi\left(r\cos\theta\frac{\partial V}{\partial r} - \sin\theta\frac{\partial V}{\partial\theta}\right)\right], \qquad (9)
\end{aligned}
$$

$\vec{\Pi}^m = \hat{u}_y V$, and V is a multiple of $e^{-jk_m r}/r$.

The dominant contributions to the electric field are from the induced electric dipoles, particularly when the radii of the spherical loading particles become small relative to the matrix propagation constant or under the condition $|k_m a| \ll 1$. Therefore one simplification that can be made is to consider only the Hertzian vector of the electric type for the electric field. This condition further simplifies the formulation by reducing the angular derivatives of the Hertz vectors to zero. The spherical components of the electric field exterior to a single loading sphere may then be written

$$
E_r = \sin\theta\cos\phi\left[\frac{\partial^2}{\partial r^2} + k_m^2\right] C\frac{e^{-jk_m r}}{r}, \qquad (10)
$$

$$
E_\theta = \cos\theta\cos\phi\left[\frac{1}{r}\frac{\partial}{\partial r} + k_m^2\right] C\frac{e^{-jk_m r}}{r}, \qquad (11)
$$

and

$$E_\phi = -\sin\phi \left[\frac{1}{r}\frac{\partial}{\partial r} + k_m^2\right] C \frac{e^{-jk_m r}}{r}. \tag{12}$$

The total field external to a single particle is the sum of the total exciting field $E(w)$ plus the scattered field due to that particle. In order to match boundary conditions on continuity of the normal electric displacement field and tangential electric field components at the surface of a particle, we must write the expressions for the electric field internal to a sphere. In this case the Hertz vectors (or Green's function) have the form of the zero-order spherical Bessel function or $\sin(k_p r)/r$ in order that the fields be finite at the center of the sphere. Therefore, with the same condition invoked that simplified eqs (8) and (9) to eqs (10) through (12), the components of the internal electric field of any sphere are

$$E_r = \sin\theta\cos\phi \left[\frac{\partial^2}{\partial r^2} + k_p^2\right] C' \frac{\sin(k_p r)}{r}, \tag{13}$$

$$E_\theta = \cos\theta\cos\phi \left[\frac{1}{r}\frac{\partial}{\partial r} + k_p^2\right] C' \frac{\sin(k_p r)}{r}, \tag{14}$$

and

$$E_\phi = -\sin\phi \left[\frac{1}{r}\frac{\partial}{\partial r} + k_p^2\right] C' \frac{\sin(k_p r)}{r}. \tag{15}$$

Application of continuity conditions on the radial component of the dielectric displacement field and on the tangential electric field gives, for $|k_m a| \ll 1$,

$$C = -\frac{a^3 E(w)[a k_p(\epsilon_m^* + 2\epsilon_p^*)\cos(k_p a) + (k_p^2 a^2 \epsilon_m^* - (\epsilon_m^* + 2\epsilon_p^*))\sin(k_p a)]}{2[k_p a(\epsilon_m^* - \epsilon_p^*)\cos(k_p a) + (k_p^2 a^2 \epsilon_m^* + \epsilon_p^* - \epsilon_m^*)\sin(k_p a)]}. \tag{16}$$

In an exactly analogous fashion, we may write the contribution to the scattered magnetic field from a single sphere under the condition $|k_m a| \ll 1$ and, by applying continuity conditions on the radial magnetic induction field and tangential magnetic field, obtain

$$D = -\frac{a^3 H(w)[k_p a(\mu_m^* + 2\mu_p^*)\cos(k_p a) + (k_p^2 a^2 \mu_m^* - (\mu_m^* + 2\mu_p^*))\sin(k_p a)]}{2[k_p a(\mu_m^* - \mu_p^*)\cos(k_p a) + (k_p^2 a^2 \mu_m^* - (\mu_m^* - \mu_p^*))\sin(k_p a)]}. \tag{17}$$

The scattered external electric and magnetic fields of any sphere located at (u, v, w) may now be written as

$$E_x^{scat} = a^3 \left[E(w) \frac{\epsilon_{a,p}^* - \epsilon_m^*}{\epsilon_{a,p}^* + 2\epsilon_m^*} (\frac{\partial^2}{\partial x^2} + k_m^2) + j\omega\mu_m^* H(w) \frac{\mu_{a,p}^* - \mu_m^*}{\mu_{a,p}^* + 2\mu_m^*} \frac{\partial}{\partial z} \right] \frac{e^{-jk_m r}}{r}, \quad (18)$$

and

$$H_y^{scat} = a^3 \left[H(w) \frac{\mu_{a,p}^* - \mu_m^*}{\mu_{a,p}^* + 2\mu_m^*} (\frac{\partial^2}{\partial y^2} + k_m^2) + j\omega\epsilon_m^* E(w) \frac{\epsilon_{a,p}^* - \epsilon_m^*}{\epsilon_{a,p}^* + 2\epsilon_m^*} \frac{\partial}{\partial z} \right] \frac{e^{-jk_m r}}{r}, \quad (19)$$

where, in general, $\mu_{a,p}^* = \mu_p^* G(k_p a)$, $\epsilon_{a,p}^* = \epsilon_p^* G(k_p a)$ are the *apparent* complex permeability and complex permittivity modified from the true complex permeability and complex permittivity by the particle inclusion penetration factor,

$$G(k_p a) = 2[\sin(k_p a) - k_p a \cos(k_p a)]/[k_p a \cos(k_p a) + (k_p^2 a^2 - 1)\sin(k_p a)]. \quad (20)$$

Note that $E(w), H(w)$ are the *total* electric and magnetic fields, which consist of the incident field (eq (1)) and the scattered fields from all *other* spheres. The total field external to any single loading spherical particle is the sum of the exciting field, which is the incident plane-wave field plus the re-radiated fields from other spheres in the matrix, and the scattered field from that particle. If the scattered fields from all the spheres on a uniform lattice are evaluated, we obtain, after some derivation, the following coupled integral equations for the total electric and magnetic field components, subject to the condition that $| k_m a | \ll 1$,

$$\begin{aligned} E_x^t(z) &= e^{-jk_m z} + \nu E_x^t(z) \frac{\epsilon_{a,p}^* - \epsilon_m^*}{\epsilon_{a,p}^* + 2\epsilon_m^*} - \frac{3}{2}\nu \int_0^\infty (jk_m \frac{\epsilon_{a,p}^* - \epsilon_m^*}{\epsilon_{a,p}^* + 2\epsilon_m^*} E_x^t(w) \\ &+ (\frac{\mu_m^*}{\epsilon_m^*})^{\frac{1}{2}} H_y^t(w) \frac{\mu_{a,p}^* - \mu_m^*}{\mu_{a,p}^* + 2\mu_m^*} \frac{\partial}{\partial w}) e^{-jk_m|w-z|} dw, \end{aligned} \quad (21)$$

$$\begin{aligned} H_y^t(z) &= (\frac{\epsilon_m^*}{\mu_m^*})^{\frac{1}{2}} e^{-jk_m z} + \nu H_y^t(z) \frac{\mu_{a,p}^* - \mu_m^*}{\mu_{a,p}^* + 2\mu_m^*} - \frac{3}{2}\nu \int_0^\infty (jk_m \frac{\mu_{a,p}^* - \mu_m^*}{\mu_{a,p}^* + 2\mu_m^*} H_y^t(w) \\ &+ (\frac{\epsilon_m^*}{\mu_m^*})^{\frac{1}{2}} E_x^t(w) \frac{\epsilon_{a,p}^* - \epsilon_m^*}{\epsilon_{a,p}^* + 2\epsilon_m^*} \frac{\partial}{\partial w}) e^{-jk_m|w-z|} dw, \end{aligned} \quad (22)$$

where $\nu = 4\pi a^3/(3d^3)$ is the volumetric loading. The three terms on the right side of eqs (21) and (22) may be identified respectively as the incident field at z, the scattered field from a spherical particle at the point z, and the scattered field from all the other particles. These equations may be solved for the effective propagation factor and impedance to give $\epsilon^*_{eff}, \mu^*_{eff}$; that is,

$$\epsilon^*_{eff} = \epsilon^*_m \left(1 + \frac{3\nu(\epsilon^*_{a,p} - \epsilon^*_m)}{\epsilon^*_{a,p}(1-\nu) + \epsilon^*_m(2+\nu)}\right), \tag{23}$$

and

$$\mu^*_{eff} = \mu^*_m \left(1 + \frac{3\nu(\mu^*_{a,p} - \mu^*_m)}{\mu^*_{a,p}(1-\nu) + \mu^*_m(2+\nu)}\right). \tag{24}$$

At least formally, eqs (23) and (24), which have a modified Maxwell-Garnett form, are consistent and correct in the dilute and dense extremes. In other words, when there is no loading ($\nu = 0$), $\epsilon^*_{eff} = \epsilon^*_m$, and $\mu^*_{eff} = \mu^*_m$. When there is vanishing host matrix ($\nu = 1, |k_p a| \gg 1$), $\epsilon^*_{eff} = \epsilon^*_p$ and $\mu^*_{eff} = \mu^*_p$.

2.2 Lorentz-Lorenz, Maxwell-Garnett, and Bruggeman Formulations

The effective dielectric and magnetic properties given by eqs (23) and (24) incorporate composite microstructure into the formalism and do not yield symmetric characterization of two-phase media. In this respect, they differ from other effective medium theories (Lorentz-Lorenz, Maxwell-Garnett, and Bruggeman) used for representing heterogeneous mixtures [7-11]. Generally, all these theories yield a mixture rule of the form

$$\frac{\psi^*_{eff} - \psi^*_m}{\psi^*_{eff} + 2\psi^*_m} = \nu_1 \frac{\psi^*_1 - \psi^*_m}{\psi^*_1 + 2\psi^*_m} + \nu_2 \frac{\psi^*_2 - \psi^*_m}{\psi^*_2 + 2\psi^*_m} + \ldots + \nu_n \frac{\psi^*_n - \psi^*_m}{\psi^*_n + 2\psi^*_m}, \tag{25}$$

where ψ^*_{eff}, ψ^*_m represent either the complex permittivity or permeability for the effective medium and the host medium, and $\psi^*_1, \psi^*_2, \ldots, \psi^*_n$ represent either the complex permittivity or permeability for the inclusions of types $1, 2, \ldots, n$. $\nu_1, \nu_2, \ldots, \nu_n$ denote the volume fractions of inclusions $1, 2, \ldots, n$. The underlying assumptions of the Lorentz- Lorenz (LL), Maxwell-Garnett (MG), and Bruggeman (B) models are also spherical inclusion geometry and dipole interactions. Spherical inclusions produce the smallest dipole moment, given the amount of particle polarizable material. The primary difference in the LL, MG, and B models is in the choice of the "host" medium. The LL approximation was essentially developed to describe point polarizable particles embedded in vacuum. In this case $\psi^*_m = 1$ so that eq (25) simply becomes

$$\frac{\psi^*_{eff}-1}{\psi^*_{eff}+2}=\nu_1\frac{\psi^*_1-1}{\psi^*_1+2}+\nu_2\frac{\psi^*_2-1}{\psi^*_2+2}. \tag{26}$$

The LL model usually is an approximation for the roughness involved in island formation film growth up to a percentage volume fraction of about 20.

The normal MG approximation corresponds to inclusions in a matrix background other than vacuum. For a two-phase medium, eq (25) then becomes

$$\frac{\psi^*_{eff}-\psi^*_m}{\psi^*_{eff}+2\psi^*_m}=\nu_1\frac{\psi^*_1-\psi^*_m}{\psi^*_1+2\psi^*_m}, \tag{27}$$

which works fairly well if the inclusions make up a small fraction of the total volume. For both the modified MG and MG formulations, different effective permittivities and permeabilities result when the roles of the matrix host and particle inclusions are interchanged, even if the respective volume fractions remain the same.

Bruggeman proposed making the properties of the matrix or host the same as the effective medium itself, yielding the following two- phase composite effective medium symmetric formulation,

$$\nu_1\frac{\psi^*_1-\psi^*_{eff}}{\psi^*_1+2\psi^*_{eff}}+\nu_2\frac{\psi^*_2-\psi^*_{eff}}{\psi^*_2+2\psi^*_{eff}}=0. \tag{28}$$

The Bruggeman formulation for a two-phase composite leads to the solution of the quadratic,

$$\psi^*_1\psi^*_2+\left(\psi^*_1(2\nu_1-\nu_2)+\psi^*_2(2\nu_2-\nu_1)\right)\psi^*_{eff}-2(\psi^*_{eff})^2=0. \tag{29}$$

Equations (23) and (24) also differ from the LL, MG, and B rules in that the loading particle permeability and permittivity properties are modified by a complex amplitude and phase wave number function that quantifies how well the field penetrates the particle. For example, the penetration factor modifies the dielectric and magnetic properties of the loading particles in accordance to the ratio of size and electrical wavelength in the spheres and is given in figure 2 as a function of $|k_p a|$. When the size of the loading spheres becomes small relative to wavelength in the sphere, $G(|k_p a|)\approx 1$. This corresponds to the case where the loading spherical inclusions are completely penetrable and $\mu^*_{a,p}=\mu^*_p, \epsilon^*_{a,p}=\epsilon^*_p$. The effective values ϵ^*_{eff} and μ^*_{eff} can be found throughout the complex plane for high particle permittivity and permeability.

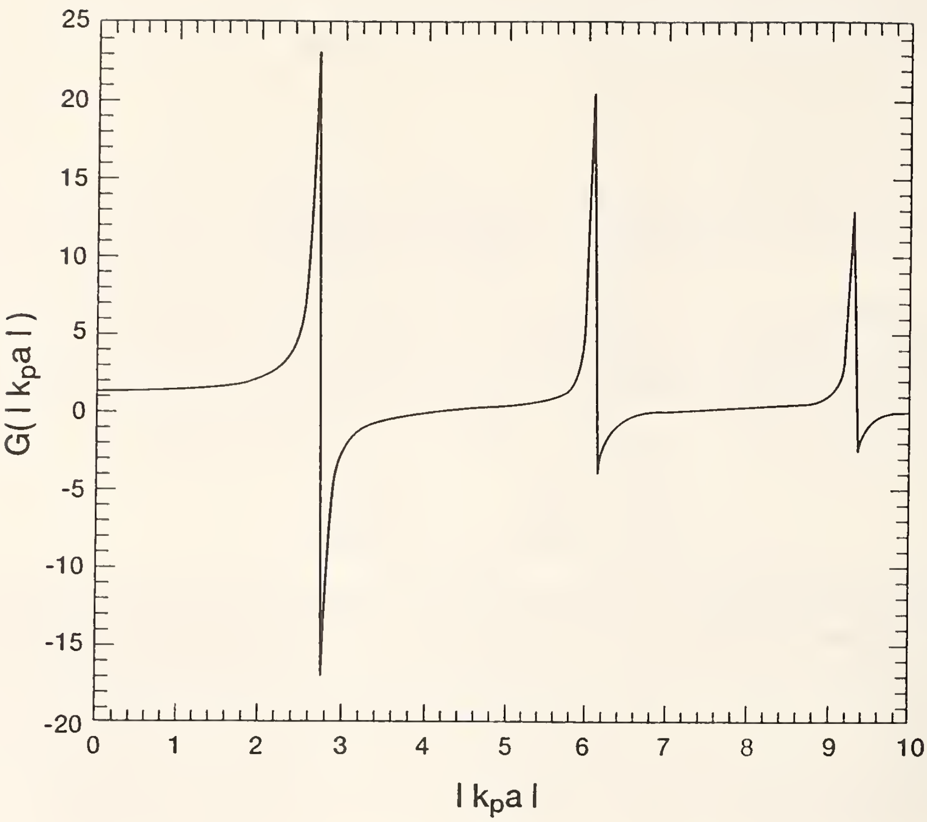

Figure 2. Penetration function modifying properties of loading particles.

3 Measurements

Over the years many methods have been developed for permittivity and permeability determination [12,13]. These methods include free-space, open-ended coaxial probe, cavity-resonators, and transmission-line techniques. Each technique has its own inherent limitations. Transmission-line techniques, usually made in rectangular or coaxial waveguides, are the simplest of the relatively accurate ways of measuring permeability and permittivity. Coaxial lines are broadband in the TEM dominant mode and therefore are attractive for spectral characterization of lossy magnetic materials, despite the problems of measurement uncertainty in complex permittivity determination introduced by potential air gaps between the sample and the coaxial line center conductor. Details of two-port, reference-plane invariant scattering parameter relations that can be used for determining permittivity and permeability are given elsewhere [13]. One set of equations for single sample dielectric and magnetic measurements from two-port scattering parameters is

$$S_{11}S_{22} - S_{21}S_{12} = \exp(-2\gamma_0(L_{air} - L))\frac{R^2 - T^2}{1 - R^2T^2}, \tag{30}$$

and

$$(S_{12}+S_{21})/2 = \exp(-\gamma_0(L_{air}-L))\frac{T(1-R^2)}{1-R^2T^2}, \tag{31}$$

where

$$R = \frac{\mu\gamma_0 - \mu_0\gamma}{\mu\gamma_0 + \mu_0\gamma}, \tag{32}$$

$$T = \exp(-\gamma L), \tag{33}$$

$$\gamma_0 = \sqrt{(\frac{2\pi}{\lambda_c})^2 - (\frac{\omega}{c_{lab}})^2}, \tag{34}$$

$$\gamma = \sqrt{(\frac{2\pi}{\lambda_c})^2 - \frac{\omega^2\mu_r^*\epsilon_r^*}{c_{vac}^2}}, \tag{35}$$

c_{vac} and c_{lab} are speed of light in vacuum and laboratory, ω is angular frequency, λ_c is cutoff transmission-line wavelength, ϵ_r^*, μ_r^* are the effective relative complex permittivity and permeability relative to vacuum, and L_{air}, L are air-line and sample lengths. Equations (30) and (31) may be solved either explicitly or implicitly as a system of nonlinear scattering equations at each frequency or by using a nonlinear regression model over the entire frequency range [14]. The respective advantages of either approach are discussed in [13]. The total attenuation loss α of a sample under test for TEM mode structure in a coaxial transmission line is given by

$$\begin{aligned} \alpha &= Re(\gamma) \\ &= Re(j\frac{\omega}{c_{vac}}\sqrt{(\epsilon_r' - j\epsilon_r'')(\mu_r' - j\mu_r'')}) \\ &= \frac{\sqrt{2}\omega}{2c_{vac}}\sqrt{\epsilon_r'\mu_r'\,[(1+\tan^2\delta_e)^{1/2}(1+\tan^2\delta_m)^{1/2} + \tan\delta_e\tan\delta_m - 1]}, \end{aligned} \tag{36}$$

where $\tan\delta_e = \epsilon_r''/\epsilon_r'$ and $\tan\delta_m = \mu_r''/\mu_r'$. Room-temperature two-port coaxial transmission-line measurements were made with a 14 mm line. Dominant TEM mode scattering-parameter data were taken with an automatic network analyzer (ANA). The ANA was calibrated such that phase measurement uncertainties were no greater than 20 millidegrees over the measurement band (1 MHz to 2 GHz); this is within the noise level of the network analyzer. Differential uncertainty analyses, which included sources of measurement error due to uncertainties in the magnitude and phase of the scattering parameters, sample holder and sample dimensions were also performed. The influence of gaps between the sample and sample holder was mitigated by conductive paste painted on the external surfaces of the sample that are in contact with the sample holder. Use of conductive paste minimizes uncertainty due to gap problems, particularly with respect to permittivity characterization. At 100 MHz, uncertainties in both permeability and magnetic loss factor determination are approximately 2 percent. The "static" or low-frequency initial permeability is well-characterized. However, low-frequency (less than 10 MHz) phase instability that is more prominent in measurements on lower-loss samples is observed in the data. For low-volumetric ferrite loading, we also see spurious mode generation at frequencies greater than 1 GHz. This is due to sample imperfections and becomes more evident on samples having lower dielectric loss.

Examples of calculated effective permittivity and permeability of ferrite-titanate mixtures whose constituents have measured room-temperature dielectric and magnetic spectra shown in figures 3, 4, and 5 are given in figures 6 and 7. These examples compare predicted effective permittivity and permeability results from the modified MG and B formalisms with measured broadband transmission line data. The predicted results used only the measured constituent data of the two-phase composite given in figures 3, 4, and 5. Generally, the measured composite data compared well with both the B and modified MG mixing rules, provided the proper matrix was chosen in the MG case. Examples of B, modified MG ferrite matrix, modified MG titanate matrix, and experimental data for permittivity and permeability at 100 MHz are shown as a function of volume percent titanate in figures 8 and 9. Generally, for low volumetric percentages of titanate, the modified MG rule worked well with the ferrite as the host matrix and the titanate particles as the guest inclusions. Similarly, for high volumetric percentages of titanate, the modified MG rule compared well with measured data with the titanate chosen as the host matrix and the ferrite particles as the guest inclusions. The B formalism yielded the best predictive permittivity and permeability values when volumetric percentages of the titanate and ferrite were approximately equal. In general, the modified MG and inverse (interchange of matrix and inclusion roles) MG rules give both lower and upper bounds for the effective permittivities and permeabilities of the composite. Overall measured magnetic dispersion for several titanate-ferrite composite mixtures is shown in figures 10 and 11. Maximal magnetic loss factors were observed at a frequency where the static initial permeability decreased by a factor of approximately one-half. In addition, the relaxation frequency increases as the volume percent titanate increases, or as the static initial permeability decreases.

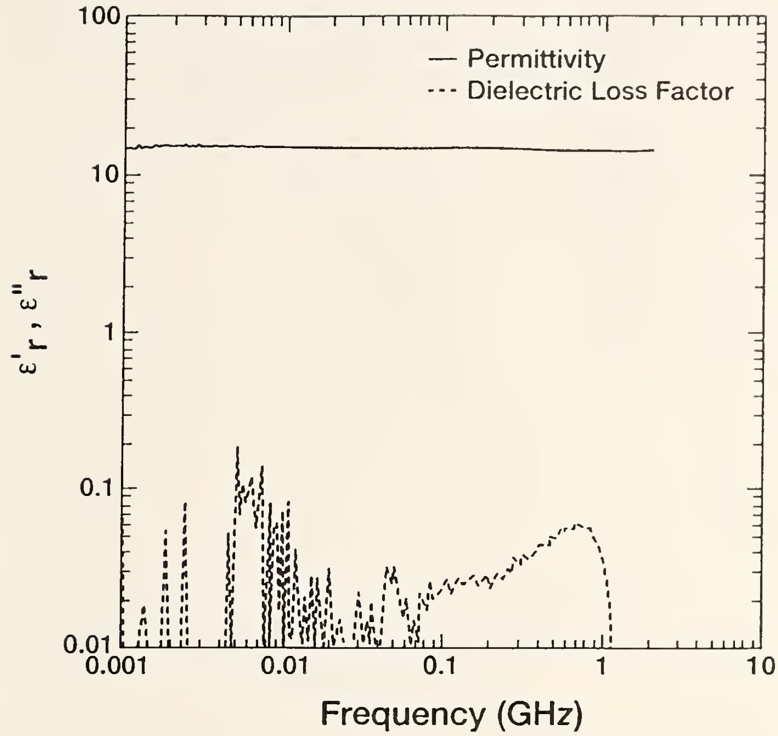

Figure 3. Measured dielectric spectra of magnesium-copper-zinc ferrite.

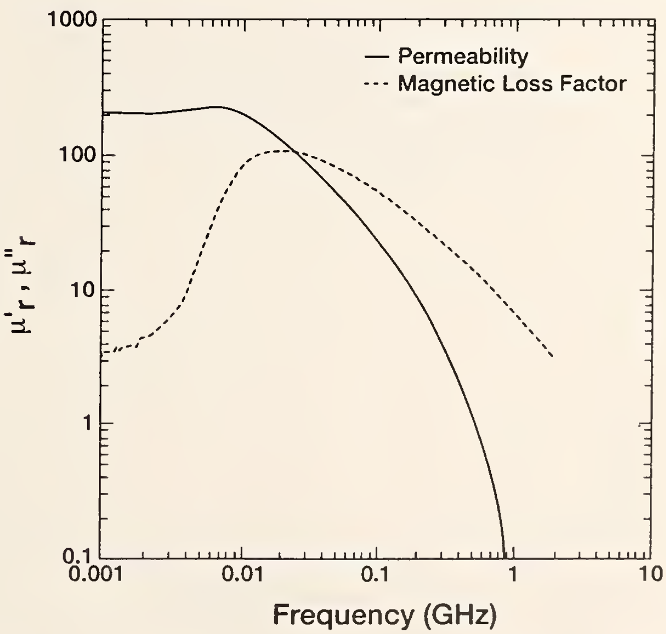

Figure 4. Measured magnetic spectra of magnesium-copper-zinc ferrite.

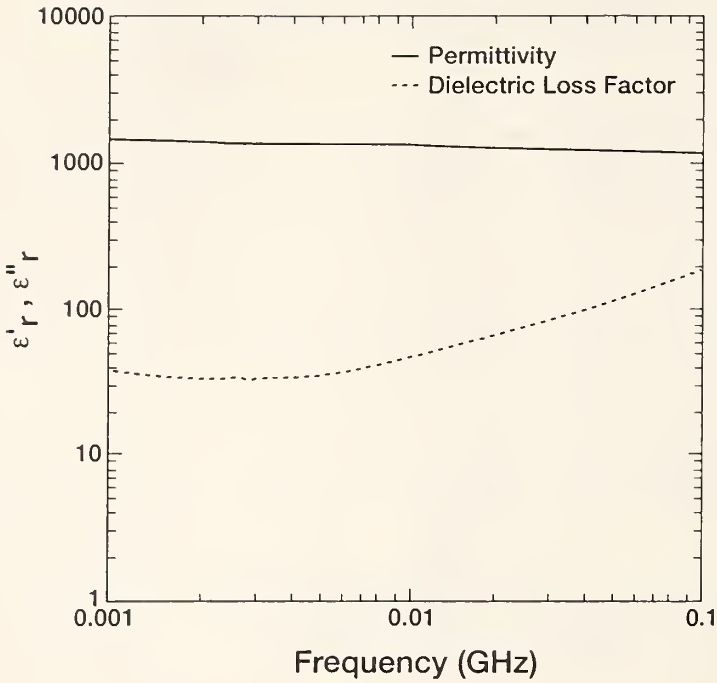

Figure 5. Measured dielectric spectra of barium titanate.

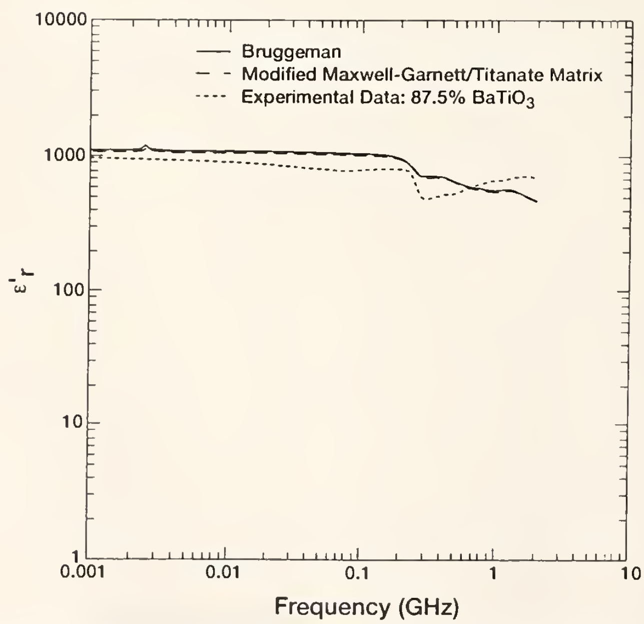

Figure 6. Spectral comparisons of ferrite-titanate composite relative permittivity with modified Maxwell-Garnett and Bruggeman predictions.

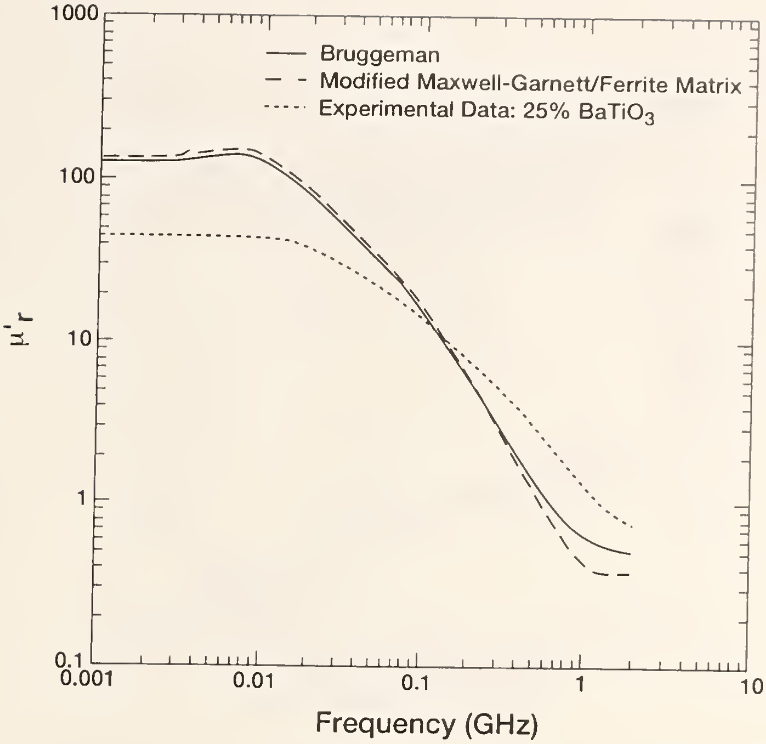

Figure 7. Spectral comparisons of ferrite-titanate composite relative permeability with modified Maxwell-Garnett and Bruggeman predictions.

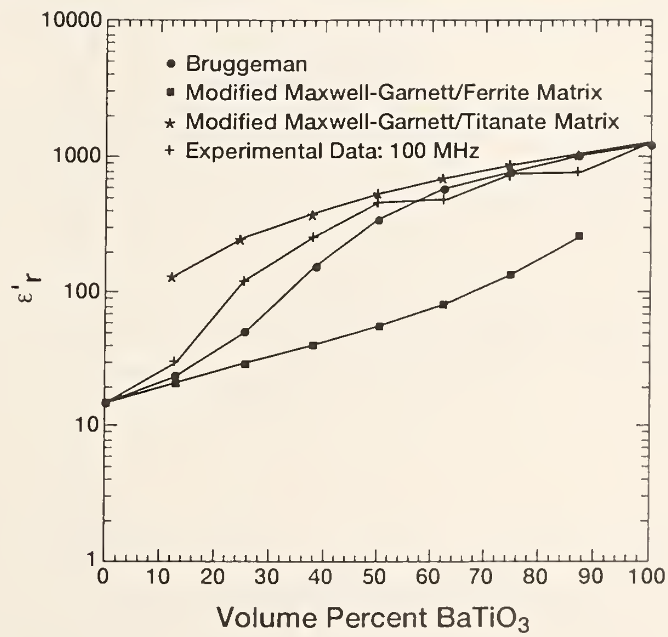

Figure 8. Permittivity of ferrite-titanate composite as a function of volume percent titanate at 100 MHz.

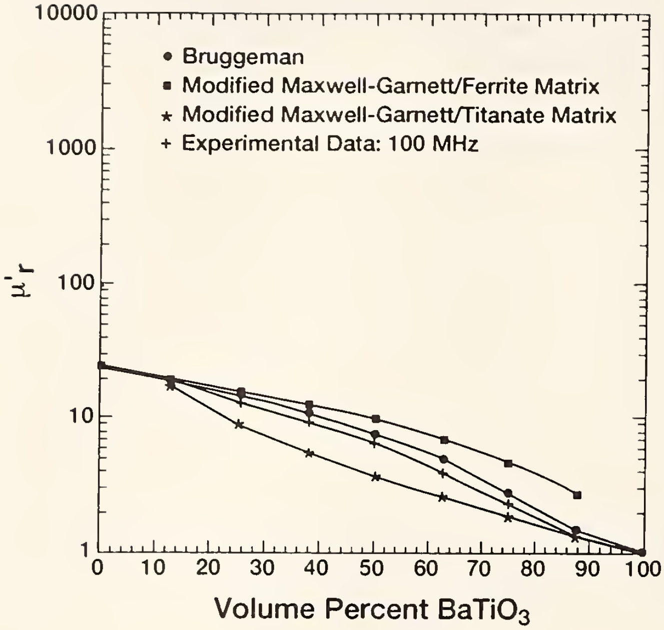

Figure 9. Permeability of ferrite-titanate composite as a function of volume percent titanate at 100 MHz.

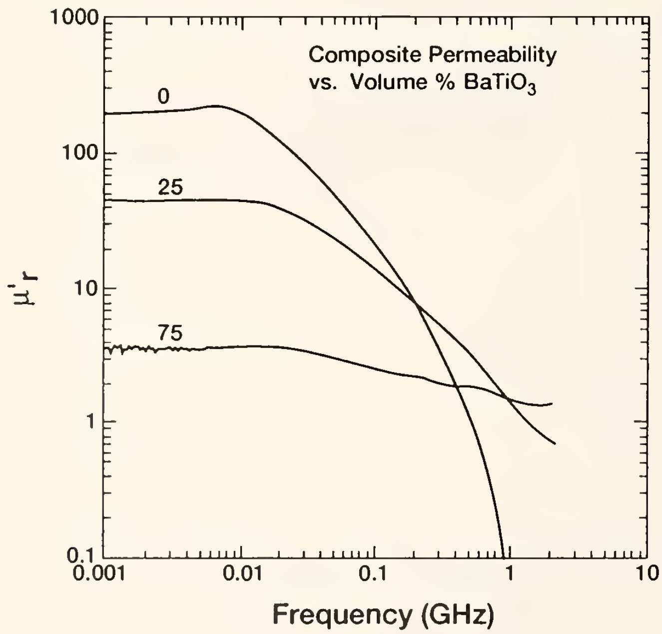

Figure 10. Measured relative permeability of ferrite-titanate composite as a function of frequency.

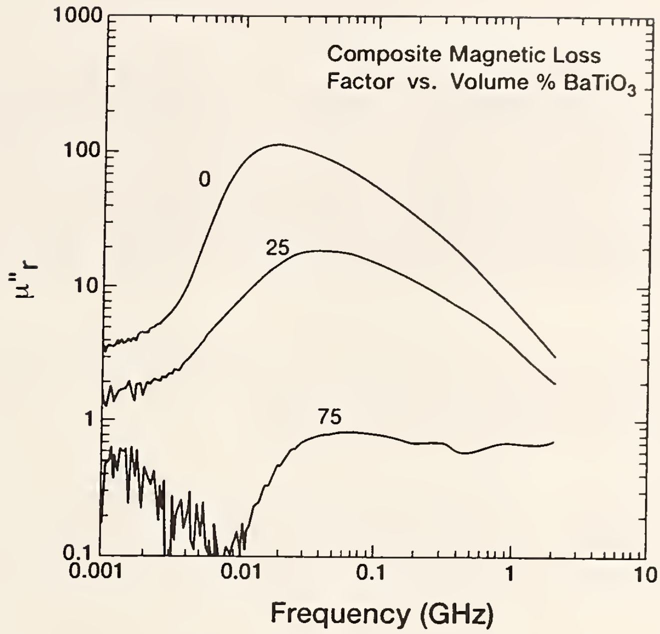

Figure 11. Measured relative magnetic loss factor of ferrite-titanate composite as a function of frequency.

4 Summary

Several approaches for predicting the spectral dielectric and magnetic behavior of heterogeneous systems have been analyzed, subject to the simplifying constraint that the loading particle radius is small relative to the wavelength in the enclosing host matrix, but not necessarily small relative to the wavelength in the loading particle. Examination of composite field behavior allows the engineering of a material's electromagnetic behavior over a broad frequency spectrum provided that the properties of the constituents can be accurately measured. Structural effects not due to special properties of the constituents may be imposed on the electromagnetic properties of the composite.

5 References

[1] Maxwell, J.C., *A treatise on electricity and magnetism.* New York: Dover, 1954.

[2] Brown, W.F., "Dielectrics," *in Handbuch der Physik*, vol. 17, S-1, Springer Verlag, Berlin, 1956.

[3] Bottcher, C.J.F. and Bordewijk, P., *Theory of electric polarization, vols. 1, 2.* New York: Elsevier, 1978.

[4] Kharadly, M.M.Z. and Jackson, W., "The properties of artificial dielectrics comprising arrays of conducting elements," Proc. IEE, vol. 66, part III, pp. 199-212, 1961.

[5] Lewin, L., "Electrical constants of spherical conducting particles in a dielectric," J. IEE (London), vol. 94, part III, pp. 65-68, 1947.

[6] Ding, K.H. and Tsang, L., "Effective propagation constants in media with densely distributed dielectric particles of multiple sizes and permittivities, "*in* Progress in electromagnetics research, vol. 1, pp. 241-295. New York: Elsevier, 1989.

[7] Aspnes, D.E., Theeten, J.B., and Hottier, F.,"Investigation of effective-medium models of microscopic surface roughness by spectroscopic ellipsometry," Phys. Rev. B, vol. 20, pp. 3292-3302, 1979.

[8] Grandquist, C.G. and Hunderi, O., "Optical properties of ultrafine gold particles," Phys. Rev. B, vol. 16, pp. 3513-3534, 1977.

[9] Landauer, R. "Electrical conductivity in inhomogeneous media" *in* "Proc. of the First Conference on Electrical Transport and Optical Properties of Inhomogeneous Media," edited by J.C. Garland and D.B. Tanner, AIP Conf. Proc. No. 40, AIP, New York, 1978.

[10] Maxwell-Garnett, J.C., "Colors in metal glasses, in metallic films, and in metallic solutions" *in* Philos. Trans. R. Soc. London, ser. A205, pp. 237-288, 1906.

[11] Bruggeman, D.A.G., "Berechnung verschiedener physikalischer Konstanten von heterogenen Substanzen," Ann. Phys. (Leipzig), vol. 24, pp. 636-679, 1935.

[12] Miles, P.A., Westphal, W.B., and Von Hippel, A., "Dielectric spectroscopy of ferromagnetic semiconductors," Rev. Mod. Phys., vol. 29, no. 3, pp. 279-307, 1957.

[13] Baker-Jarvis, J., Janezic, M., Grosvenor, J., and Geyer, R.G., "Transmission/reflection and short circuit line methods for permittivity and permeability determination," Natl. Inst. Stand. Technol. Note 1355, 1992.

[14] Baker-Jarvis, J., Geyer, R.G., and Domich, P., "A nonlinear least-squares solution with causality constraints applied to transmission line permittivity and permeability determination," IEEE Trans. Instrum. Meas., vol. 41, no. 5, pp. 646-652, 1992.

*U.S. GOVERNMENT PRINTING OFFICE:1994-673-018/00053

NIST *Technical Publications*

Periodical

Journal of Research of the National Institute of Standards and Technology—Reports NIST research and development in those disciplines of the physical and engineering sciences in which the Institute is active. These include physics, chemistry, engineering, mathematics, and computer sciences. Papers cover a broad range of subjects, with major emphasis on measurement methodology and the basic technology underlying standardization. Also included from time to time are survey articles on topics closely related to the Institute's technical and scientific programs. Issued six times a year.

Nonperiodicals

Monographs—Major contributions to the technical literature on various subjects related to the Institute's scientific and technical activities.

Handbooks—Recommended codes of engineering and industrial practice (including safety codes) developed in cooperation with interested industries, professional organizations, and regulatory bodies.

Special Publications—Include proceedings of conferences sponsored by NIST, NIST annual reports, and other special publications appropriate to this grouping such as wall charts, pocket cards, and bibliographies.

Applied Mathematics Series—Mathematical tables, manuals, and studies of special interest to physicists, engineers, chemists, biologists, mathematicians, computer programmers, and others engaged in scientific and technical work.

National Standard Reference Data Series—Provides quantitative data on the physical and chemical properties of materials, compiled from the world's literature and critically evaluated. Developed under a worldwide program coordinated by NIST under the authority of the National Standard Data Act (Public Law 90-396). NOTE: The Journal of Physical and Chemical Reference Data (JPCRD) is published bi-monthly for NIST by the American Chemical Society (ACS) and the American Institute of Physics (AIP). Subscriptions, reprints, and supplements are available from ACS, 1155 Sixteenth St., NW, Washington, DC 20056.

Building Science Series—Disseminates technical information developed at the Institute on building materials, components, systems, and whole structures. The series presents research results, test methods, and performance criteria related to the structural and environmental functions and the durability and safety characteristics of building elements and systems.

Technical Notes—Studies or reports which are complete in themselves but restrictive in their treatment of a subject. Analogous to monographs but not so comprehensive in scope or definitive in treatment of the subject area. Often serve as a vehicle for final reports of work performed at NIST under the sponsorship of other government agencies.

Voluntary Product Standards—Developed under procedures published by the Department of Commerce in Part 10, Title 15, of the Code of Federal Regulations. The standards establish nationally recognized requirements for products, and provide all concerned interests with a basis for common understanding of the characteristics of the products. NIST administers this program in support of the efforts of private-sector standardizing organizations.

Consumer Information Series—Practical information, based on NIST research and experience, covering areas of interest to the consumer. Easily understandable language and illustrations provide useful background knowledge for shopping in today's technological marketplace.

Order the **above** *NIST publications from: Superintendent of Documents, Government Printing Office, Washington, DC 20402.*

Order the **following** *NIST publications—FIPS and NISTIRs—from the National Technical Information Service, Springfield, VA 22161.*

Federal Information Processing Standards Publications (FIPS PUB)—Publications in this series collectively constitute the Federal Information Processing Standards Register. The Register serves as the official source of information in the Federal Government regarding standards issued by NIST pursuant to the Federal Property and Administrative Services Act of 1949 as amended, Public Law 89-306 (79 Stat. 1127), and as implemented by Executive Order 11717 (38 FR 12315, dated May 11, 1973) and Part 6 of Title 15 CFR (Code of Federal Regulations).

NIST Interagency Reports (NISTIR)—A special series of interim or final reports on work performed by NIST for outside sponsors (both government and non-government). In general, initial distribution is handled by the sponsor; public distribution is by the National Technical Information Service, Springfield, VA 22161, in paper copy or microfiche form.

U.S. Department of Commerce
National Institute of Standards and Technology
325 Broadway
Boulder, Colorado 80303-3328